e-Polymers **2011**, no. 010

http://www.e-polymers.org

ISSN 1618-7229

Functional nano fillers in epoxy-dicyandiamide adhesives for prolonged shelf life and efficient cure

Jan Christoph Gaukler,[1] *Ulrich Müller,*[2] *Jan Kristian Krüger,*[2] *Wulff Possart*[1*]

[1*]Saarland University, Chair of Adhesion & Interphases in Polymers, Campus C6.3, PB 151150, 66041 Saarbruecken, Germany; fax: 0049 681 302 4960; e-mail: w.possart@mx.uni-saarland.de
[2] Luxembourg University, Campus Limpertsberg, 162A, avenue de la faïencerie, 1511 Luxembourg; fax: 00352 466644 6329; e-mail: jan-kristian.kruger@uni.lu.

(Received: 13 April, 2010; published: 01 March, 2011)

Abstract: Shelf life at room temperature and curing behaviour at elevated temperature are studied for hot-curing accelerated epoxies (EP, diglycidylether of bisphenol A plus dicyandiamide (Dicy)) by FTIR-spectroscopy and modulated DSC. The accelerator is added either directly or with nano-zeolite filler to the EP. Due to the immobilisation of the accelerator in the pores of the nano-zeolite, the shelf life of this EP is 5 times longer than for the EP containing free accelerator. While the free accelerator acts during the whole heating step to curing temperature, the nano-zeolite does not release the accelerator before ca. 100 °C. As monitored by light microscopy, the released accelerator not only supports the curing but also stimulates the dissolution of the solid Dicy. As the result, network formation at 170 °C finishes within less than 25 minutes for the nano-filled EP.

Introduction

Many epoxy formulations (EP) contain dicyandiamide (Dicy) as a multi-functional curing agent - Figure 1. In addition, they often contain an accelerator like tertiary amines, phenol derivatives, urea derivatives or imidazoles for a lower curing temperature and time [7-11]. Unfortunately, all accelerators reduce the shelf life of the formulation at room temperature.

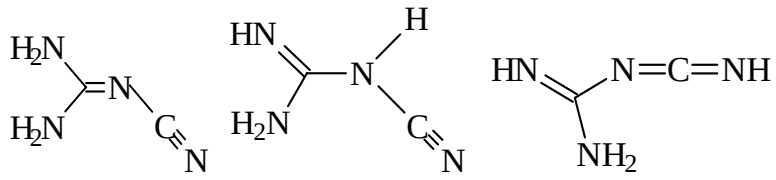

Fig. 1. Tautomeric structures of Dicyandiamide (Dicy) according to [1-6].

Several authors [12-15] tried to solve this problem by latent hardeners or accelerators like tertiary amines blocked with modified novolaks, metal ions or coordination compounds. For example, it was found that a Cu(II)-imidazole complex features a very good shelf life at room temperature [16-18]. Smith [19] investigated coordination compounds containing acetylacetonate ligands as latent accelerators in anhydride-cured EP resins. He attested a very good shelf life (> six months) and found very short gelation times at curing temperatures between 150 °*C* and 175 °*C*.

As another approach, the accelerator is encapsulated in a polymer shell (e.g. micrometer-sized imidazole particles coated with an adapted polysiloxane shell, [20]). For curing, the temperature is raised above the softening point of the shell (ca. 160 °*C* for this polysiloxane) where it releases the accelerator in a controlled way. The shell material, the blocking compounds or the ligand molecules remain in the EP network.

As a new approach, a very reactive accelerator was immobilized in µ-zeolite particles (size distribution 400-1200 *nm*, average size ≈ 600 *nm* [22]) via a sorption process. Therefore the zeolite was optimised with respect to structure (pore size) and host-guest interactions. The thermal release behaviour was characterised in air [21]. The µ-zeolite reversibly immobilizes the accelerator. In the EP, the immobilisation should result in two effects. First, it should prevent the accelerator from mixing with the EP system at room temperature. In thermal curing, Second, the µ-zeolite particles should release the accelerator in a well-defined range of curing temperature. As compared to the EP without accelerator, the network should form either at lower temperature or within reduced curing time at increased temperature. In our previous study [23], the loaded µ-zeolite was added to an EP adhesive (diglycidylether of bisphenol A (DGEBA, DER 332) and dicyandiamide (Dicy, Dyhard®100SF, Dicy content: 96.3 weight-%), mass ratio 100 : 7) and stored at 25 °*C* in regular air or cured (heating rate β = 10 *K / min* to 170 °*C* and subsequent isothermal curing for 45 *min*). Shelf life and curing behaviour were investigated by FTIR-spectroscopy and modulated DSC. At 25 °*C*, the shelf life of the EP with the loaded µ-zeolite is three times the shelf life of the EP with free accelerator. The free accelerator acts from the beginning of the heating process at room temperature but the loaded µ-zeolite releases the accelerator at about 76 °C. Network formation in the filled EP finishes at 170 °*C* after not more than 19 *min*. In spite of that nice combination of storage and curing properties which is a proof of concept, the µ-zeolite particles do not provide a very uniform distribution of released accelerator in the EP matrix. Moreover, the obtained features in terms of shelf life and accelerated curing are promising but not fully satisfying for practical applications.

Therefore, a nano-zeolite (size < 500 *nm*) is considered in this paper. It is tailored as host system for accelerators by computer simulations at Fraunhofer IFAM (Bremen, Germany) and prepared by NanoScape (Martinsried, Germany). IFAM also loaded that new nano-material with an accelerator and characterized the release in air and in technically relevant EP formulations.

As a first goal, this study is devoted to the release mechanism. The EP mixed with free accelerator (= EP_{accel}) is compared with the nano-zeolite filled system (= $EP_{n\text{-}filled}$) containing the same concentration of accelerator. That condition determines the amount of nano-filler in this epoxy formulation. It was not tested to what maximum concentration the nano-zeolites can be incorporated. According to studies with silica particles of similar size [24, 25] the loading limit of epoxy formulations is certainly not exceeded. The $EP_{n\text{-}filled}$ possesses a low viscosity and good handling. Moreover, the chemical modifications during storage at 25 °*C*, the curing process and the resulting network state are compared for the two EP formulations on the basis of experimental data obtained with IR spectroscopy and temperature modulated DSC (TMDSC). The curing of EP adhesive without and with accelerator is monitored by polarised light microscopy for studying the influence of the accelerator.

Results and discussion

Shelf life of EP_{accel} and $EP_{n\text{-}filled}$

Uncured samples of EP_{accel} and $EP_{n\text{-}filled}$ were stored at 25 °*C* in ambient air and studied by ATR IR spectroscopy after selected time intervals. The little decrease of the epoxy band at 915 cm^{-1} and the slight increase of the ether band at 1105 cm^{-1} are monitored (Figures 2, 3). These simultaneous changes verify the formation of oligoether chains via a mechanism similar to an anionic polymerization and that is initiated by the accelerator-epoxy zwitterionic adduct [7].

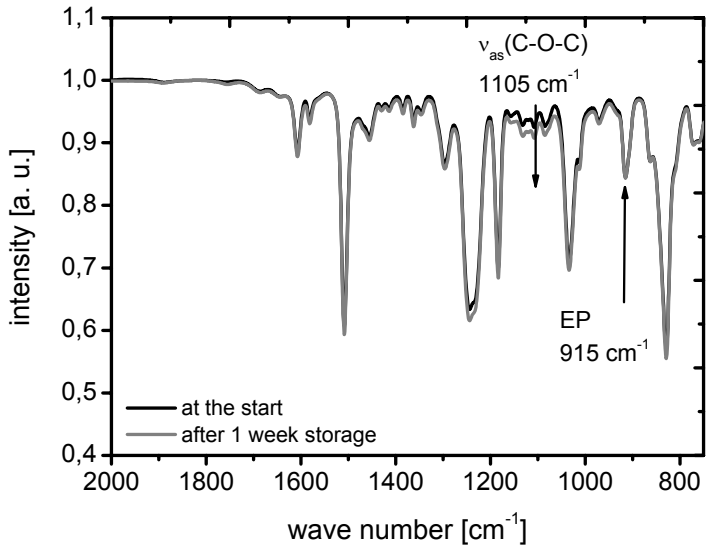

Fig. 2. IR spectra (2000 cm^{-1} - 750 cm^{-1}) of EP_{accel} after 7 days storage at 25 °*C*.

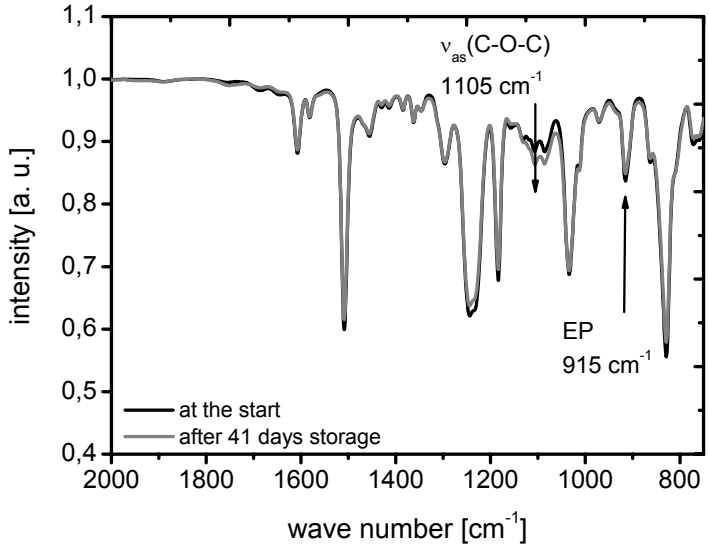

Fig. 3. IR spectra (2000 cm^{-1} - 750 cm^{-1}) of $EP_{n\text{-}filled}$ after 41 days storage at 25 °*C*.

The oligoether fraction at $t_{storage}$ is quantified as the difference of the corresponding oxirane content and the oxirane content at $t_{storage} = 0$, i.e. immediately after prepolymerization. Then, the change of epoxy consumption $\Delta U_{EP}^{spectr}\left(t_{prepoly}, t_{storage}\right)$ due to oligoether formation in the prepolymer is calculated from the normalized peak height of the band at 915 cm^{-1} by

$$\Delta U_{EP}^{spectr}\left(t_{prepoly}, t_{storage}\right) = \left(\frac{I_{915}^{norm}\left(1\ h, t_{storage} = 0\ d\right) - I_{915}^{norm}\left(1\ h, t_{storage}\right)}{I_{915}^{norm}\left(t_{prepoly} = 0\ h, t_{storage} = 0\ d\right)} \right) \cdot 100\ \% \qquad (1)$$

as given in Figure 4. The rate of epoxy consumption and hence of the polyether content is significantly higher for EP_{accel} than for $EP_{n\text{-}filled}$. Here the shelf life is defined as the limit for appropriate handling in the laboratory due to viscosity increase. It corresponds to $\Delta U_{EP}^{spectr} = 15\%$ in the adhesive. Due the loaded nano-zeolite fillers, the shelf life of $EP_{n\text{-}filled}$ exceeds the small value of EP_{accel} by 49 days. Nevertheless, this result shows that there is a slow release of accelerator molecules from the nano-zeolite into the epoxy resin.

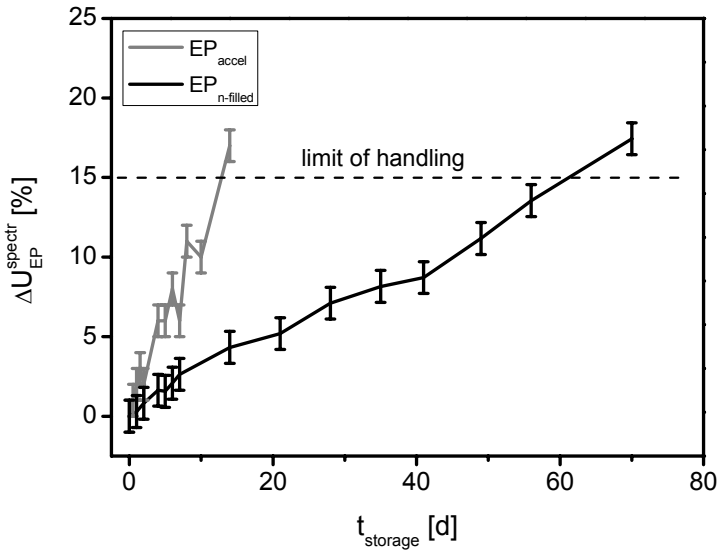

Fig. 4. Oxirane consumption $\Delta U_{EP}^{spectr}\left(t_{storage}\right)$ due to the formation of oligoether sequences during storage at room temperature. The bars indicate the experimental error.

Influence of the accelerator on the curing

The influence of the accelerator on the dissolution of Dicy crystallites is revealed by polarized light microscopy. Therefore, microscopic as well as macroscopic Dicy crystals are grown from solution in methanol on glass slides. These crystals are immersed in DGEBA (Figure 5) and in DGEBA plus accelerator (Figure 6). Then, the regular temperature program for curing (heating with 10 *K / min* to 170 °*C*) is applied. The temperature at which the microscopic crystals start to dissolve is taken a characteristic of the dissolution process. For both samples, i.e. Dicy in DGEBA and Dicy in DGEBA plus accelerator, the relevant microscopic crystalline structure is encircled in white. For the system Dicy/DGEBA, the first signs of dissolution of

microscopic crystalline structures were observed at ca. 83 °*C* (= 356 *K*). In DGEBA containing the accelerator the dissolution already starts at ca. 58 °*C* (= 331 *K*). This 25 *K* shift of the onset of dissolution is a clear indication for its promotion by the accelerator.

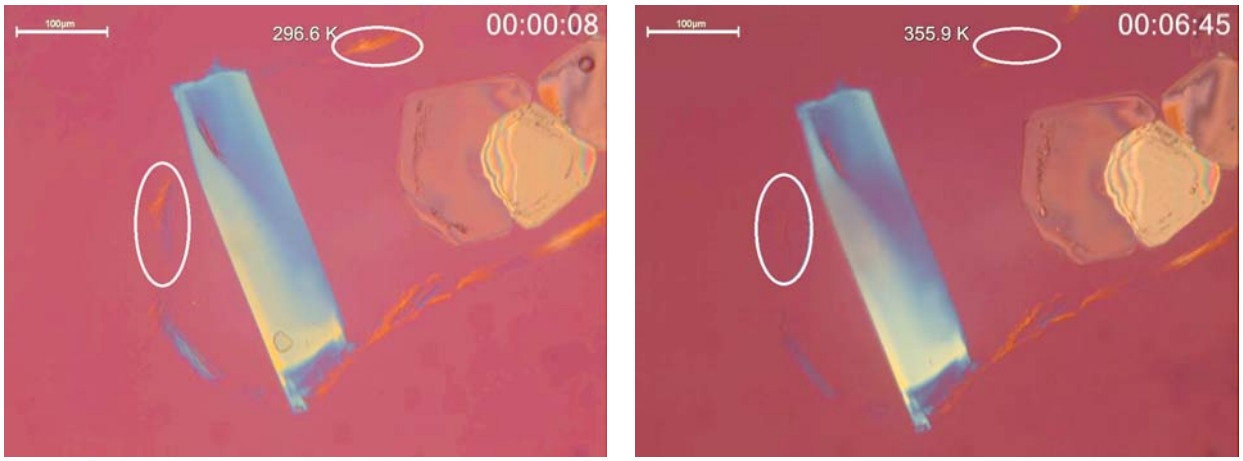

Fig. 5. Dicy crystals in DGEBA with the initial state (left) and with a snapshot of the first occurrence of crystal dissolution (right). The white circles denote the regions of interest for the discussion.

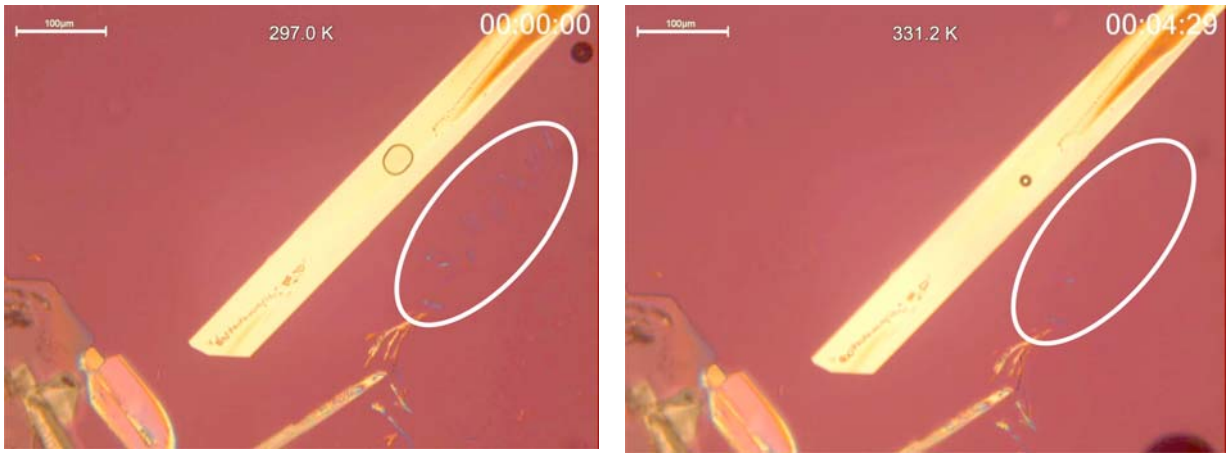

Fig. 6. Dicy crystals in DGEBA plus accelerator: The left-hand picture displays the Initial state (left) and snapshot of the first occurrence of crystal dissolution (right). White circles denote the regions of interest for the discussion.

Curing of EP_{accel} and $EP_{n\text{-}filled}$

For EP_{accel} samples, the oxirane consumption starts at about 100 °*C* – Figure 7. In the graph, the curing time scale starts (t_{cure} = 0 *min*) when T = T_{cure} = 170 °*C* is reached. The negative curing times correspond to the heating period to 170 °*C*. The corresponding oxirane conversion U_{EP}^{spectr} is calculated from the normalized peak height of the band at 915 cm^{-1} by

$$U_{EP}^{spectr}\left(t_{prepoly}, t_{cure}\right) = \left(\frac{I_{915}^{norm}\left(t_{prepoly} = 0\ h, t_{cure} = 0\ min\right) - I_{915}^{norm}\left(t_{prepoly} = 1\ h, t_{cure}\right)}{I_{915}^{norm}\left(t_{prepoly} = 0\ h, t_{cure} = 0\ min\right)} \right) \cdot 100\ \% \qquad (2)$$

In EP_{accel}, the oxirane consumption accelerates at about 120 °*C* (i.e. at t_{cure} = -5 *min*) after starting at 100 °C (t_{cure} = -7 *min*). Due to this high reaction rate, almost all oxirane rings have been consumed when the sample reaches the isothermal curing at 170 °*C*. In contrast, U_{EP}^{spectr} starts at 125 °C (t_{cure} = -4.5 *min*) in the $EP_{n\text{-}filled}$ samples, reaches only 67 *%* at 170 °*C* and needs circa another 20 *min* at 170 °*C* to complete.

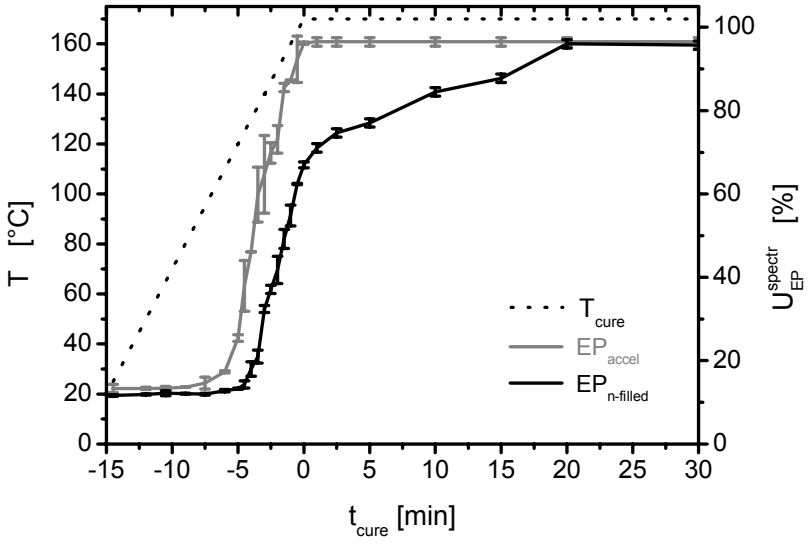

Fig. 7. Oxirane conversion in EP_{accel} and $EP_{n\text{-}filled}$ during curing. The bars indicate the experimental error.

For the primary amine groups of Dicy, the characteristic band (1575 cm^{-1}, Figure 8) starts growing at 95 °*C* in EP_{accel} but not before 120 - 125 °*C* in $EP_{n\text{-}filled}$ samples. For the nitrile groups (2172 cm^{-1}, Figure 9), the band intensity starts to increase at 95 °*C* in EP_{accel} and at 120 °*C* in $EP_{n\text{-}filled}$. That simultaneous increase of Dicy band intensities is related to the information depth of the ATR IR spectroscopy. Accordingly, only Dicy molecules in the surface layer of the sample (ca. 3 *µm* thick) contribute to the spectra. Hence at low temperature, only some part of Dicy crystals is seen in the spectra. As soon as Dicy molecules start to dissolve into the liquid DGEBA with rising temperature, their average concentration grows in the ATR information volume. In the ATR IR spectra, this growth is monitored as long as the dissolution rate exceeds the curing rate in the EP network at the given temperature.

Indeed, the rate of oxirane consumption also grows with temperature (cf. Fig. 7). The oxirane rings react with the amine groups [8, 11, 26-35]. At some temperature, their consumption exceeds the supply of Dicy molecules from the dissolving particles. That results in the maxima for $I_{1575}^{norm}(t_{cure})$ at 125 °*C* and 135 °*C* for EP_{accel} and $EP_{n\text{-}filled}$, respectively (Fig. 8). Hydroxyl groups appear as the result of that addition reaction. They provide the reaction partner for the nitrile groups [8, 11, 26-35] - Figure 10. Therefore, the curves for $I_{2172}^{norm}(t_{cure})$ also go through maxima at ca. 125 °*C* and 140 °*C* for EP_{accel} and $EP_{n\text{-}filled}$, respectively (Fig. 9).

This interpretation of the spectroscopic features for $EP_{n\text{-}filled}$ agrees well with the Dicy dissolution behaviour monitored by light microscopy. The release of accelerator from the nano-zeolite particles becomes chemically effective above about 120 °*C*.

Concerning the end of curing, the following conclusions can be drawn from Figs. 8, 9. While primary amine groups (I_{1575}^{norm}) vanish at t_{cure} = 0 *min* in EP_{accel}, another 2.5 *min* at 170 °*C* are needed in $EP_{n\text{-}filled}$ to consume that species. Full consumption of nitrile groups of dissolved Dicy goes on at 170 °*C* for five minutes ($t_{cure} \approx 5$ *min*), both in EP_{accel} and $EP_{n\text{-}filled}$.

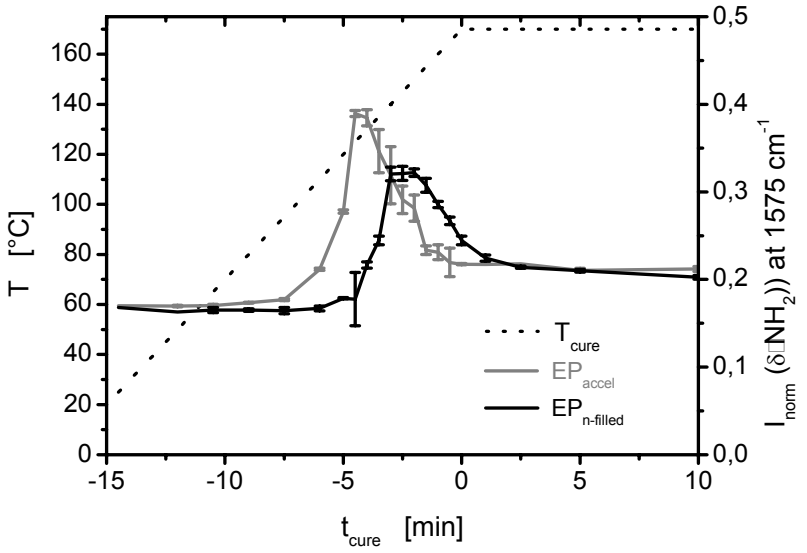

Fig. 8. Normalized intensity of the δ(NH_2) band at 1575 cm^{-1} during the curing of EP_{accel} and $EP_{n\text{-}filled}$. The bars indicate the experimental error.

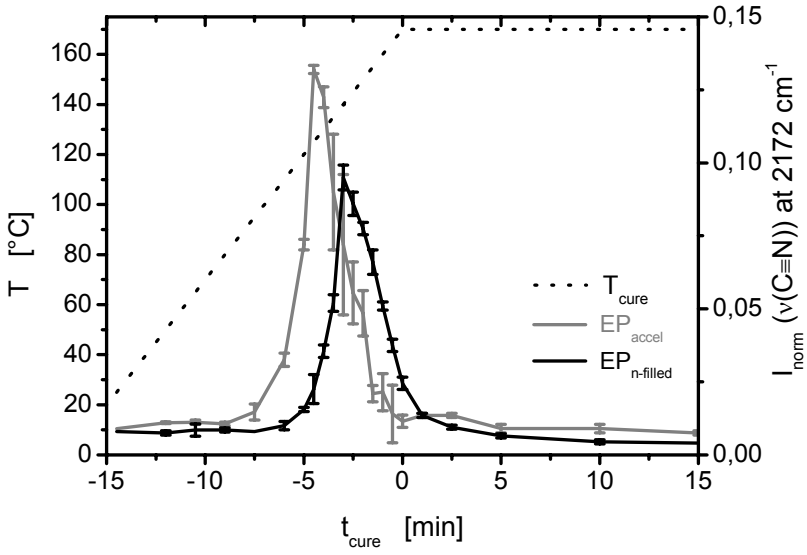

Fig. 9. Normalized intensity of the δ(C≡N) band at 2172 cm^{-1} during the curing of EP_{accel} and $EP_{n\text{-}filled}$. The bars indicate the experimental error.

It is interesting to note that another nitrile band at 2208 cm^{-1} still exists after curing – Figure 11. This wave number points to nitrile groups in residual solid Dicy particles.

The existence of such residuals is verified on electron micrographs of fracture faces of cured samples [36].

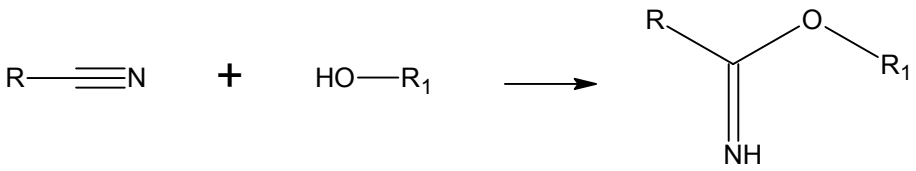

Fig. 10. Reaction of nitrile and hydroxyl groups.

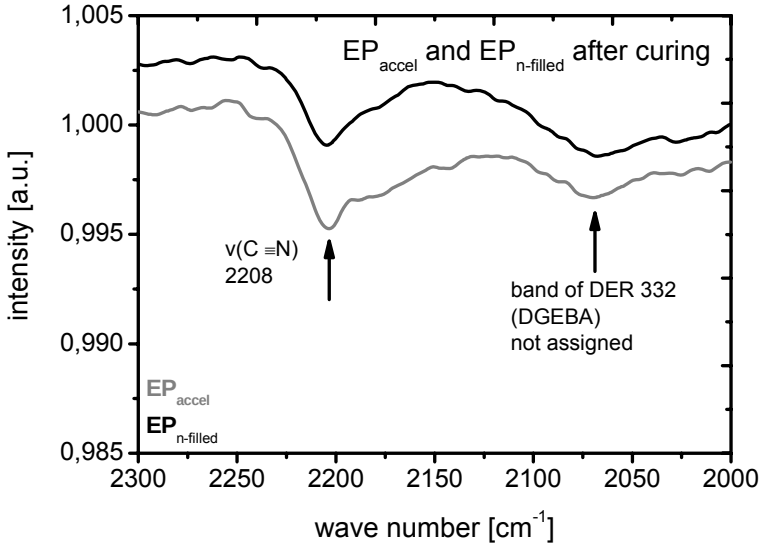

Fig. 11. IR spectra (2300 cm^{-1} - 2000 cm^{-1}) of EP_{accel} and $EP_{n\text{-}filled}$ after curing.

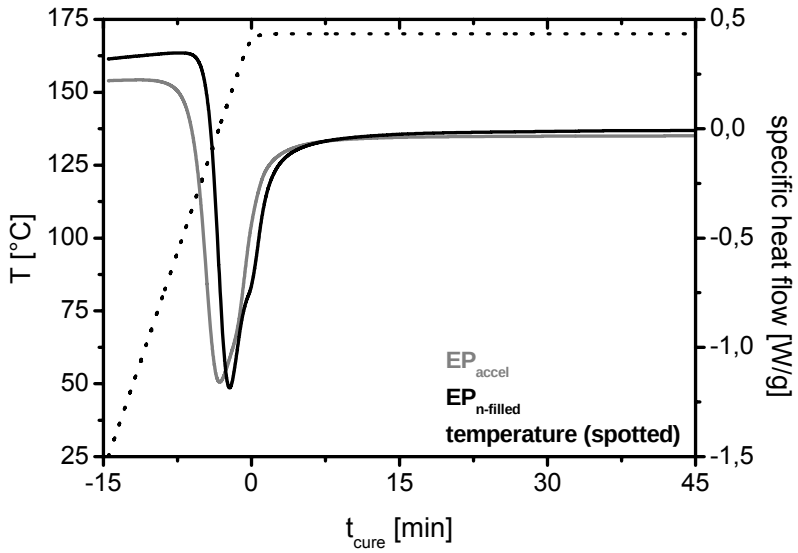

Fig. 12. MDSC of the curing of EP_{accel} and $EP_{n\text{-}filled}$ for β = 10 *K / min.*

That result is of practical importance. Note that in both EPs the Dicy amount is less than the stoichiometric mass ratio which ranges from 100 : 9.9 to 100 : 12.4, depending on the details of the curing mechanism [31-35]. Hence, the full oxirane consumption observed here implies that the oxirane rings do not react with amine groups only: They polymerize via the accelerator-epoxy zwitterionic adduct and they add to hydroxyl groups that originate from the reaction of oxirane rings and amine groups. Both reaction paths result in ether joints.

The MDSC results complement the spectroscopic characterization very well – Figures 12-14:

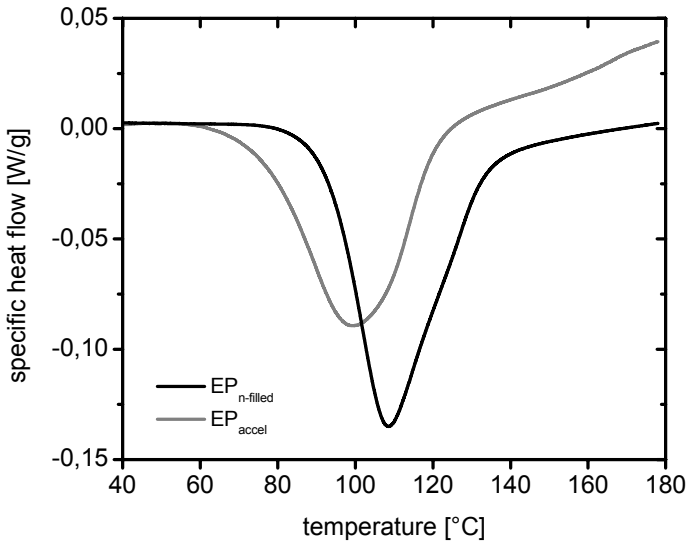

Fig. 13. MDSC specific heat flow of the curing of EP_{accel} and $EP_{n\text{-}filled}$ for $\beta = 0.5\ K / min$.

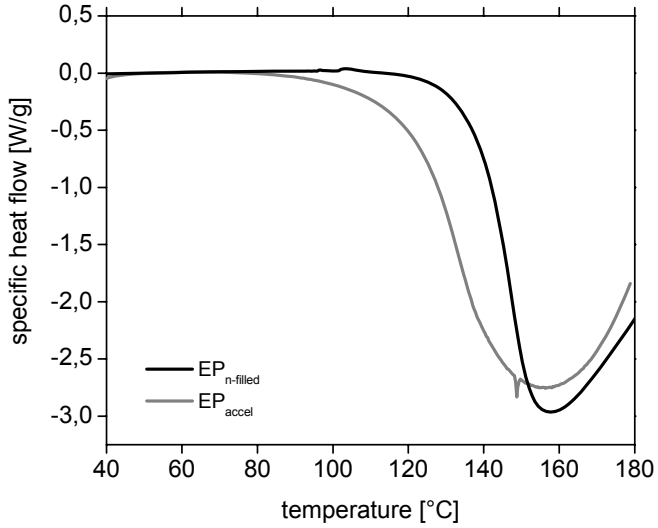

Fig. 14. MDSC specific heat flow of the curing of EP_{accel} and $EP_{n\text{-}filled}$ for $\beta = 20\ K / min$.

Compared to EP_{accel}, $EP_{n\text{-}filled}$ start to cure at an increased temperature depending on the heating rate (Tab. 1). Consequently, the nano-zeolite releases the accelerator at a higher temperature than 25 °C. Then, the cure of $EP_{n\text{-}filled}$ proceeds faster (as monitored by the maximum of heat release – Tab. 2) and finishes slightly later than for EP_{accel}.

Tab. 1. Start of heat release depending on the heating rate.

	Heating rate 0.5 *K / min*	**Heating rate 10 *K / min***	**Heating rate 20 *K / min***
EP_{accel}	50 °C	61 °C	65 °C
$EP_{n\text{-}filled}$	77 °C	100 °C	109 °C

Tab. 2. Maximum of heat release depending on the heating rate.

	Heating rate 0.5 *K / min*	**Heating rate 10 *K / min***	**Heating rate 20 *K / min***
EP_{accel}	99 °C	138 °C	156 °C
$EP_{n\text{-}filled}$	108 °C	149 °C	157 °C

The zeolites visibly influence the chemical vitrification during heating with β = 0.5 *K / min* (Figure 15).

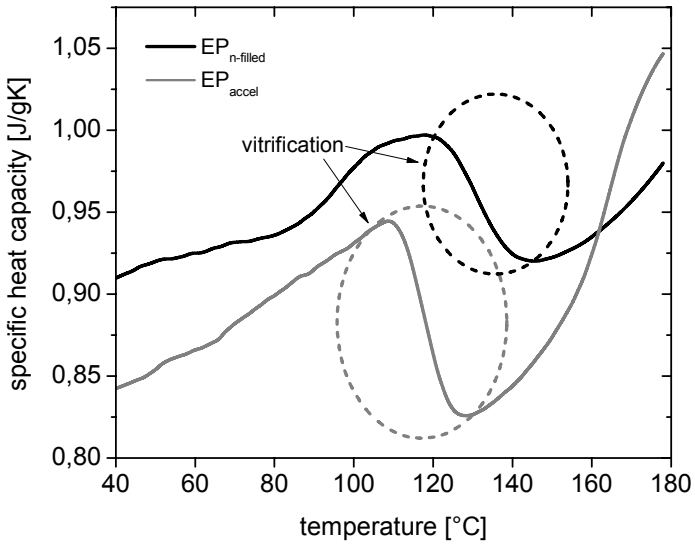

Fig. 15. MDSC specific heat capacity of the curing of EP_{accel} and $EP_{n\text{-}filled}$ for β = 0.5 *K / min*.

The vitrification appears as a step in the specific heat capacity. The step goes in the opposite direction, however the formation of cross-links during the heating process drives the system into the glassy state, i.e. the glass transition temperature increases faster with chemical conversion and time than the sample temperature during heating. Vitrification occurs for EP_{accel} at T_{vit} = 118 °*C* and for $EP_{n\text{-}filled}$ at T_{vit} = 131 °*C*. In the course of the vitrification, the reactions slow down until a rising temperature is

able to deliberate the system from the glassy state again, yielding a positive step in the specific heat capacity then. This step is broad because the glass transition temperature shifts further due to the chemical reactions and the increase of temperature with time.

All TMDSC results confirm the very fast curing of the two adhesive formulations and the high activity of the used accelerator.

Calorimetric characterization of the samples after curing with 10 $K \cdot min^{-1}$ provides a similar glass transition with the same $T_g = 172\ °C \pm 2\ K$ for both adhesives – Figure 16. That is a first indication for the similarity of the resulting epoxy networks but this aspect deserves further study.

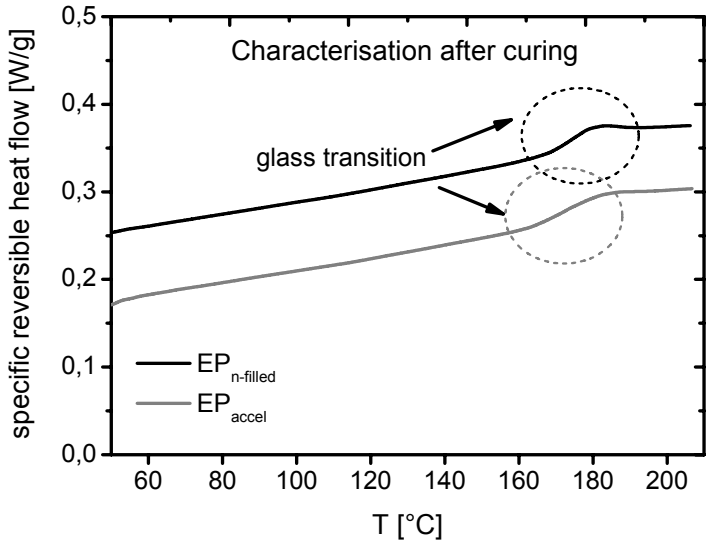

Fig. 16. MDSC characterisation of EP_{accel} and $EP_{n\text{-}filled}$ with β = 10 *K / min* after curing at 170 °*C* for 45 *min.*

Conclusions

In contrast to the EP system containing free accelerator, the accelerator-loaded nano-zeolite provides a fivefold shelf life time at 25 °*C*. According to our previous results [23], accelerator-loaded nano-zeolite is superior to accelerator-loaded µ-zeolites which grant a threefold shelf time only. The nano-zeolite features a controlled release of the accelerator at a defined temperature which depends on the heating rate ($T_{start\ of\ cure}^{\beta = 0.5\ K/min} = 77\ °C$, $T_{start\ of\ cure}^{\beta = 10\ K/min} = 100\ °C$, $T_{start\ of\ cure}^{\beta = 20\ K/min} = 109\ °C$ in MDSC).

The released accelerator is not only directly involved in the chemical reaction path of the epoxy network formation. As a new result, it is shown by light microscopy that the accelerator promotes the dissolution of the crystalline Dicy (starting at ca. 120 °*C* for 10 $K \cdot min^{-1}$). For 10 $K \cdot min^{-1}$ heating rate, the oxirane conversion starts to rise at 100 °*C* for the epoxy with free accelerator while this rise shifts to 120 °*C* in the system with accelerator-loaded nano-zeolite. Thus the combination of the two steps of (a) accelerator release, which may be Arrhenius-like, and (b) stimulation of Dicy dissolution by the released accelerator provides a pseudo-barrier behaviour for the loaded nano-zeolite. Then, oxirane rings, nitrile and amine groups are quickly consumed when the epoxy systems reach 170 °*C*. The loaded nano-zeolite filler

results in an efficient cure at 170 °*C*. The network formation is completed within the short time period of max. 23 *min*. In conclusion, the goal of reducing the curing temperature by such a filled zeolite to 130 °*C* appears to be realistic.

Experimental part

Preparation of the epoxies

The epoxy system consists DGEBA (Figure 17, CAS-Nr. 1675-54-3; DOW, DER 332) and Dicy (CAS-Nr. 461-58-5; Alzchem Trostberg GmbH; Dyhard®100SF, Dicy content: 96.3 weight-%) in the mass ratio 100 : 7.

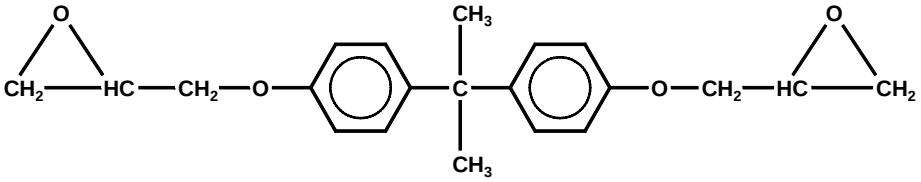

Fig. 17. Diglycidylether of bisphenol A (DGEBA).

The micronized solid Dicy tends to precipitate in the liquid DGEBA. Therefore, the epoxy mixture was pre-cured at 150 °*C* for 1 *h*. This step partially dissolved the Dicy and the reaction with DGEBA formed oligomers. The corresponding IR spectroscopic oxirane conversion was 15 *%*. The increased viscosity of that prepolymer avoids Dicy sedimentation. It is degassed in vacuum and homogenized in a Speedmixer® (3200 min^{-1}, 2 x 30 *s*, Hauschild Engineering, DAC 150 FV) in normal air at 40 °*C* to form EP. For EP_{accel}, the accelerator (0.5 *%* by weight, substance not revealed for proprietary reasons) was added to EP by mixing in the Speedmixer under the same conditions. $EP_{n\text{-}filled}$ was obtained by dispersing the loaded nano-zeolite filler (2.9 *%* by weight which corresponds to 0.5 *%* by weight of accelerator) in the prepolymer EP.

Temperature Modulated DSC

TMDSC investigations in a Q100 calorimeter (TA Instruments) were carried out at a heating rate β = 10 $K{\cdot}min^{-1}$ with sinusoidal temperature modulation at f = 1 / 60 *Hz* and an amplitude ΔT = 1 *K*. The measuring cycle for network formation started by heating the samples (6 *mg* in Au-coated Al pans) with β from 5 °*C* to 170 °*C*, then, isothermal curing followed for 45 *min*. It was finished by cooling down to 25 °*C* with - 10 $K{\cdot}min^{-1}$. The glass transition of the network was deduced from the reversible specific heat flow measured on the cured samples during a second heating from 25 °*C* to 225 °*C* with β and the same modulation parameters. In additional measurements, the heating rate was varied on a modified calorimeter DSC822e (Mettler Toledo) with a sample mass of ca. 10 *mg*. For β = 0.5 $K{\cdot}min^{-1}$, f = 1 / 120 *Hz* and ΔT = 0.5 *K* are used. For β = 20 $K{\cdot}min^{-1}$, no modulation was applied. The samples were heated from 30 °*C* to 180 °*C*. The temperature of chemical vitrification was determined as the inflection point of the step in the specific heat capacity.

FTIR spectroscopy

Two types of samples were prepared in Au-coated Al pans to monitor curing by IR spectroscopy. As the first type, samples were heated in N_2 atmosphere with

10 $K \cdot min^{-1}$ from 25 °*C* to selected temperatures between 25 °*C* and 170 °*C* and quenching (β = - 60 $K \cdot min^{-1}$) to room temperature followed immediately. The second type of samples was heated to 170 °*C* in the same way and annealed at 170 °*C* for selected times between 0 and 45 *min* before quenching to 25 °*C*.

Viscous samples were removed from the pans and measured by a FTIR spectrometer **Bruker** IFS 66v/s in the ATR mode (Attenuated Total Reflection, Harrick Seagull reflection unit, ZnSe hemisphere, p-polarized light, angle of incidence 65°, spectra information depth from 0.3 *µm* at 4000 cm^{-1} to 2.8 *µm* at 400 cm^{-1}). Hard samples were investigated in their pans by an ATR FTIR microscope Hyperion (µ-ATR, Bruker, IR-ATR 20x objective, lateral resolution: 80 *µm*, Ge crystal, p-polarized light, angle of incidence 30°, information depth: 0.3 *µm* @ 4000 cm^{-1} - 3.5 *µm* @ 400 cm^{-1}). The single beam sample spectra were divided by the single beam reference spectrum of the atmosphere. The influence of temporal variations of humidity was minimized by purging the customized sample compartment with dried air (dew point: -70 °*C*, CO_2 content < 200 *ppm*). For the µ-ATR IR spectra, the atmospheric compensation function implemented in the spectrometer software was applied to eliminate small residual bands from H_2O and CO_2.

For the quantitative analysis of curing, the peak heights of the epoxy ring (915 cm^{-1}) and of the nitrile group (ν (-C≡N) = 2172 cm^{-1}) were considered. The primary amine groups only form a shoulder (δ (-NH_2) = 1570 cm^{-1}) on the phenyl band at 1580 cm^{-1} which is not involved in curing. Therefore, the decrease of peak height at 1580 cm^{-1} was taken as an indirect measure of the concentration change of primary amine groups. All band intensities were divided by the peak height of the well separated phenyl band at 1510 cm^{-1} as internal standard:

$$I_{xxx}^{norm} = \frac{I_{xxx}}{I_{1510}} \qquad (3)$$

Light microscopy

Samples were prepared in a two-step process. First, Dicy crystals were grown from solution in methanol on microscope slides. Then the crystals were covered with a layer of DGEBA with or without accelerator. These samples were closed by cover slides.

The optical investigation was performed in a Leica Pol-S microscope with crossed polarizers and a lambda-filter for phase contrast. The temperature program (heating with 10 $K\ min^{-1}$ to 170 °*C*) was realised with a LINCAM thermostat.

The point of disappearance of microscopic crystals (<20 *µm*) was taken as the thermal onset of the dissolution of Dicy.

Acknowledgements

This study was funded by the German Federal Ministry of Education and Research (BMBF) within the project FKZ 03X0026.

References

[1] Jones, W. J.; Orville-Thomas, W. J. *Transactions of the Faraday Society*, Faraday Society and Contributors, **1959**, *55*, 193.

[2]Robert, C. W.; Melvin, J. A. in: Lide, D. R. and Milne, G. W. A. (eds.): *Handbook of Data on Organic Compounds*, CRC, **1985**, 465.
[3]Boerio, F. J., Hong, P. P., *Materials Science and Engineering*, **1990**, *A126*, 245-252
[4]Gaillard, F.; Romand, M.; Verchère D.; Hocquaux, H. *Journal of Adhesion*, **1994**, *46*, 227.
[5]Hong, S. G.; Wang, T. C. *Journal of Applied Polymer Science*, **1994**, *52 (9)*, 1339.
[6]Bengu, B.; Boerio, F. J. *Journal of Adhesion*, **2006**, *82*, 1133.
[7]Ashcroft, W.R. in Ellis, B. (Ed.), *Chemistry and Technology of Epoxy Resins*, **1993**, 37.
[8]Güthner, T.; Hammer, B. *Journal of Applied Polymer Science*, **1993**, *50 (8)*, 1453.
[9]Lin, Y.G.; Sautereau, H.; Pascault, J.P. *Journal of Polymer Science*, *Part A: Polymer Chemistry*, **1986**, *24 (9)*, 2171.
[10] Poisson, N.; Maazouz, A.; Sautereau, H.; Taha, M.; Gambert, X. *Journal of Applied Polymer Science*, **1998**, *69 (12)*, 2487.
[11] Saunders, T.F., Levy, M.F., Serino, J.F. *Journal of Polymer Science, Part A-1*, **1967**, *5*, 1609.
[12] Sanftenberg, H.; Fedtke, M. *Die Angewandte Makromolekulare Chemie*, **1995**, *225 (3942)*, 99.
[13] Dowbenko, R.; Anderson, C.C.; Chang, W.-H. *Industrial and Engineering Chemistry Product Research and Development*, **1971**, *10 (3)*, 344.
[14] Kurnoskin, A.V. *Polymer - Plastics Technology*, **1994**, *33 (2)*, 175.
[15] Hamerton, I.; Howlin, B. J.; Jepson, P. *Coordination Chemistry Reviews*, **2002**, *224*, 67.
[16] Barton, J.M.; Hamerton, I.; Howlin, J.B.; Jones, J.R. *Polymer Bulletin*, **1994**, *33*, 347.
[17] Barton, J.M.; Hamerton, I.; Howlin, J.B.; Jones, J.R.; Liu, S. *Polymer*, **1998**, *39 (10)*, 1929.
[18] Buist, G.J.; Hamerton, I.; Howlin, J.B.; Jones, J.R.; Liu, S.; Barton, J.M. *Journal of Materials Chemistry*, **1994**, *4 (12)*, 1793.
[19] Smith, J.D.B. *Journal of Applied Polymer Science*, **1981**, *26 (3)*, 979.
[20] Cao, M.; Xie, P.; Zhong, J.; Zhang, Y.; Zhang, R.; Chung, T.-S.; He, C. *Journal of Applied Polymer Science*, **2002**, *85 (3)*, 873.
[21] Gröppel, P.; Schlosser, T.; Noeske, M.; Faupel, F.; Geiß, P.L. *WING – Das Jahrbuch 2008*, **2008**, 354.
[22] Daniell, W. *private communication, CEO NanoScape AG, Planegg-Martinsried, Germany.*
[23] Gaukler, J. C.; Müller, U.; Krüger, J. K.; Possart, W. *Composite Interfaces*, **2010**, *17 (8),* 743.
[24] Sanctuary, R.; Baller, J.; Zielinski, B.; Becker, N.; Krüger, J. K.; Philipp, M.; Müller, U.; Ziehmer, M. *Journal of Physics: Condensed Matter*, **2009**, 21 (3), art. no. 035118.
[25] Baller, J.; Becker, N.; Ziehmer, M.; Thomassey, M.; Zielinski, B.; Müller, U.; Sanctuary, R. *Polymer*, **2009**, 50 (14), 3211.
[26] Sacher, E. *Polymer* **1973**, *14 (3)*, 91.
[27] Zahir, S. A. *Advances in Organic Coatings Science and Technology* **1982**, 4, 83.
[28] Gilbert M. D.; Schneider, N. S.; MacKnight, W. J. *Macromolecules* **1991**, 24 (2), 360.
[29] Fedtke, M.; Domaratius, F.; Walter, K.; Pfitzmann, A. *Polymer Bulletin* **1993**, 31, 429.

[30] Pfitzmann, A.; Fliedner, E.; Fedtke, M. *Polymer Bulletin* **1994**, *32*, 311.
[31] Fata, D.; Bockenheimer, C.; Possart, W. *Epoxies on Stainless Steel - Curing and Aging*, in: Adhesion - Current Research and Application, Possart, W. Ed., **2005**, 479.
[32] Fata, D.; Possart, W. *Journal of Applied Polymer Science*, **2006**, *99*, 2726.
[33] Fata, D. *Epoxidsysteme im Verbund mit rostfreien Stählen – Vernetzung und Alterung (Epoxies in Composites of Stainless Steels – Curing and Ageing)*, Dissertation, Saarland University, Germany, published by Shaker; **2007**
[34] Devriendt, O. Curing *and Ageing of Hot Curing Epoxy Adhesives: An XPS-Study*, Study Research Report, Saarland University and University of Surrey, Germany and United Kingdom, **2009**.
[35] Gaukler, J. C.; Devriendt, O.; Marino P.; Watts, J. F.; Possart, W. *Proceedings*, 4th World Conference on Adhesion and Related Processes WCARP 2010, Arcachon, France, **2010**.
[36] Dufloux, C. *Strukturbildung und Morphologie Dicyandiamid-basierter Epoxidklebstoffe (Structure Formation and Morphology of Epoxy Adhesive Based on Dicyandiamide),* Diploma thesis, Chair of Adhesion and Interphases in Polymers, Saarland University, **2008**.